BIGLOBAL INSTABILITIES OF STEADY AND PULSATILE FLOWS IN A 75% AXISYMMETRIC STENOTIC TUBE

Spencer Sherwin[1] and Hugh Blackburn[2]
[1]Department of Aeronautics, Imperial College London,UK
[2]CSIRO Manufacturing and Infrastructure Technology, Australia

INTRODUCTION

Atherosclerosis, the formation of plaques within the arterial wall, continues to be a major cause of death in the developed world. The associated narrowing, or stenosis, of the artery can lead to potential significant restriction of blood flow to downstream vessels. Related to this condition is the potential of plaque ruptures and thrombosis formation leading to particles becoming lodged in smaller vessels possibly inducing myocardinal infarction or stroke.

This association of arterial disease with flow related mechanisms, such as wall shear stress variation, has motivated the study of steady and pulsatile flow within both model and anatomically correct arterial model stenoses [1]. Under standard physiological flow conditions most arterial flows are usually considered to be laminar, although typically separated and unsteady. However in the case of a stenotic flow the the increase in local Reynolds number at a contraction can lead to transitional flow associated with the early stages of turbulence. The occurrence of turbulent like flow phenomena makes the numerical simulation of these flows particularly challenging especially when considering the large range of parameters required to describe both the geometrical and flow features.

An efficient methods to analyse these types of flow is simplified geometries is using Biglobal stability analysis. Biglobal stability analysis is the numerical determination of the linearised stability of the two-dimensional flow state. The computational cost associated with this method is primarily associated with the cost of computing the two-dimensional flows. Therefore it provides a computationally efficient approach to understanding the stability of flows over a range of parameters for a comparatively small cost when compared to full three-dimensional unsteady flow simulations. Previously [2] we have applied this method to understand the stability of stenotic channels. In the current work we turn our attention to the linearised stability of steady and pulsatile flow in an axisymmetric stenotic tube.

NUMERICAL METHODOLOGY

Governing equations and parameter space

We consider the flow in our stenotic tube (see fig 1) to be governed by the incompressible Newtonian Navier-Stokes equations

$$\frac{\partial \mathbf{u}}{\partial t} = -\mathbf{N}(\mathbf{u}) - \frac{1}{\rho}\nabla p + \frac{1}{Re}\nabla^2 \mathbf{u} \qquad \nabla \cdot \mathbf{u} = 0 \tag{1}$$

where $\mathbf{u}$ is the three dimensional velocity field, ρ and p are the fluid density and pressure respectively, and Re is the Reynolds number $Re = \overline{u}D/\nu$. In the following problem we will take our length scale D as the pipe diameter and base the Reynolds number on the temporally and spatially average inflow velocity $\overline{u}$. $\mathbf{N}(\mathbf{u})$ is the nonlinear advection operator $\mathbf{N}(\mathbf{u}) = (\mathbf{u} \cdot \nabla)\mathbf{u}$ and equation (1) is subject to no-slip boundary conditions at the walls, a prescribed velocity at the inflow (steady or periodic), conditions of zero pressure and zero outward normal derivatives of velocity at the outflow and consistent regularity boundary conditions at the axis as explained in [3].

The axisymmetric stenosis shown in fig 1 is described by a sinusoidal stenotic shape which can be described by two geometric parameters: The stenosis degree $S = 1-(D_{\min}/D)^2$ and the stenosis length $\lambda = L/D$. In the following study we have considered the geometry defined by $S = 0.75$ and $\lambda = 2$.

To complement the geometric factors we also need to consider the physiological flow parameters which describe our problem. If we permit the inflow to have a pulsatile waveform of period T and restrict our attention to cases of non-reversing, spatially averaged flow we can identify three important flow parameters: The Reynolds number, Re; the Womersley number, $\alpha = (D^2\pi/(2\nu T))^{1/2}$ and the peak to mean flow ratio $Q_{p2m} = Q_{\text{peak}}/Q_{\text{mean}}$, where Q is the mass flux. The Womersley number can be interpreted as the ratio of the diameter (or radius) to the viscous boundary layer growth in time period T which is the ratio of two sectional length scales. An alternative parameter commonly used in fluid mechanics is the reduced velocity $U_{red} = \overline{u}T/D$ which is the ratio of the convective length the mean flow moves in time T to the diameter. For geometries where there is a length scale in the flow direction, as is the case of the stenosis, this non-dimensional parameter can prove to be a useful alternative to the Womersley number. We note that U_{red} and α are dependent parameters related by the Reynolds number according to $U_{red} = \pi Re/(2\alpha^2)$.

BiGlobal stability analysis

Following the formulation in [4, 5, 3] we set up our bigobal stability problem by decomposing the instantaneous flow field into a two-dimensional base flow, $\mathbf{U}$, and a small perturbation $\mathbf{u}'$:

$$\mathbf{u}(x,r,\theta,t) = \mathbf{U}(x,r,t) + \mathbf{u}'(x,r,\theta,t) \tag{2}$$

$\mathbf{U}$ is an axisymmetric solution of equation (1) which by definition is invariant in the θ-direction in cylindrical coordinates. Inserting the decomposition (2) into (1) and neglecting quadratic we obtain the linearised Navier-Stokes equations:

$$\frac{\partial \mathbf{u}'}{\partial t} = -\mathbf{DN}(\mathbf{u}') - \frac{1}{\rho}\nabla p' + \frac{1}{Re}\nabla^2 \mathbf{u}' \tag{3}$$

where $\mathbf{DN}$ is the linearised advection operator and $\mathbf{u}'$ is divergence free with zero Dirichlet boundary conditions on the inflow and outer wall. At the outflow and along the axis we enforce the same outflow conditions as imposed previously

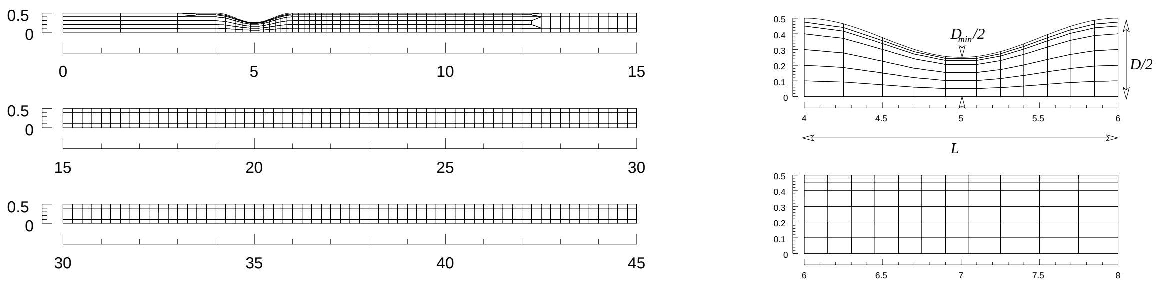

Figure 1: Macro spectral element computational mesh on meridional semi-plane. Thefull computational domain was extended to $x = 50D$ with a similar mesh structure to that shown at $x = 45D$.

on $\mathbf{u}$. A further simplification to the form of $\mathbf{u}'$ can be made due to homogeneity of the domain in the θ direction by expressing the perturbation as a Fourier expansion, i.e.

$$\mathbf{u}'(x, r, \theta, t) = \sum_{\beta=-\infty}^{\beta=\infty} \hat{\mathbf{u}}_\beta(x, r, \beta, t) e^{i\beta\theta} \tag{4}$$

Applying the Fourier transform, equation (3) can be written more compactly as:

$$\frac{\partial \hat{\mathbf{u}}_\beta}{\partial t} = \mathbf{L}(\hat{\mathbf{u}}_\beta, \beta) \tag{5}$$

where the linear operator $\mathbf{L}(\hat{\mathbf{u}}_\beta, \beta)$ represents the Fourier transform of the right hand side of (3) and is dependent on the base flow $\mathbf{U}$.

Solutions of (5) comprise a sum of exponential functions of the form $\hat{\mathbf{u}}_\beta(x, r) e^{i\beta\theta} e^{\sigma t}$. When the flow is time periodic the modes $\hat{\mathbf{u}}_\beta$ are referred to as the 'Floquet eigenfunctions' of operator $\mathbf{L}$. For steady base flows we consider the exponents σ and a mode is linearly unstable (will grow in time) if the real part of this exponent is greater than zero. Equivalently, in the study of periodic flows we generally consider the 'Floquet multipliers', $\mu = e^{\sigma T}$, which give a measure of the growth of the perturbation mode throughout one base flow cycle. The corresponding mode becomes unstable if the magnitude $|\mu|$ becomes greater than unity; if μ leaves the unit circle in the complex plane.

Defining the operator $\mathbf{A}$ which describes the evolution of $\mathbf{u}'$ over the period T as

$$\mathbf{A}(\hat{\mathbf{u}}) = \exp\left(\int_0^T \mathbf{L}(\hat{u}) dt \right) \tag{6}$$

The Floquet multipliers are the eigenvalues of $\mathbf{A}$, and the eigenmodes of $\mathbf{A}$ correspond to the Floquet eigenfunctions. In the case of steady base flow then an arbitrary time period T is chosen for computational convenience and the relevant exponents reclaimed via the relation $\sigma = (\ln(\mu)/T)$.

Numerical Methods

Both the Navier-Stokes equations for the base flow and the linearised Navier-Stokes equations for the perturbation field were solved using the cylindrical coordinate implementation of the spectral element equations [3]. This solver uses a Lagrange tensor product expansion based upon the Gauss-Lobatto-Legendre quadrature points together with a velocity correction splitting scheme to discretise the Navier-Stokes solver[6]. Fig 1 shows the 743 macro elements used to discretise the solution within which which a polynomial expansions or order 7 were applied make a total of 47,552 local degrees of freedom per variable.

The eigenvalues of $\mathbf{A}$ were evaluated using an Arnoldi method which requires the time integrating equations of (3) at every iteration. Further details of this approach can be found in [4, 5, 3]. The Arnoldi iteration was converged to a tolerance of at least $1e^{-6}$ on all calculations.

RESULTS AND DISCUSSION

Biglobal stability of Steady Flow

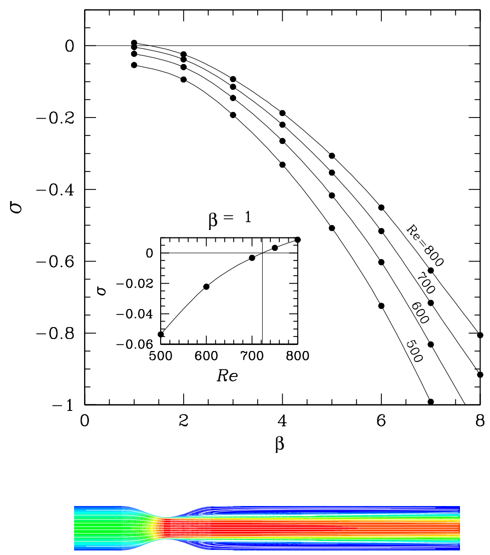

Figure 2: Top figure indicated the variation of σ with azimuthal wavenumber β for different Reynolds numbers. Bottom figure shown the base flow streamlines and axial velocity at Re=722.

In figure 2 we see a snapshot of the base flow at $Re = 722$ showing the streamline pattern of the separated flow immediately after the stenotic region. The inset of the top plot in figure 2 shows the leading real part of the eigenvalue, σ, as a function of Reynolds number at an azimuthal wave number of $\beta = 1.0$. From this plot we observe that the critical Reynolds number for growth of the linearised perturbation occurs at a Reynolds number of $Re = 722 \pm 1$. Also shown in the top plot of figure 2 is the the real part of the maximum eigenvalue as a function of azimuthal wavenumber β where we observe that the case of $\beta = 1$ is the most unstable azimuthal wavenumber.

BiGlobal stability of Pulsatile flow

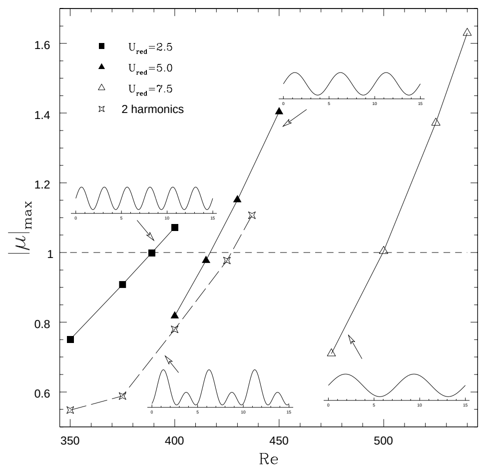

Figure 3: Plot of largest absolute Floquet multiplier, $|\mu|_{max}$ for reduced velocities of $U_{red} = 2.5, 5.0$ and 7.5 as well as the multiple waveform using two harmonics

In figure 3 we show the results of a biglobal stability analysis for a range of different pulsatile flows as indicated by the inset plots. Most of the velocity waveforms contained a single harmonic and are of the form $u_m(t) = 1.0 + 0.75 \sin(2\pi t/U_{red})$ with $U_{ref} = 2.5, 5.0, 7.5$. A two harmonic waveform was also considered and with a velocity waveform $u_m(t) = 1.0 + 0.75(\sin(2\pi t/U_{red}) - \cos(4\pi t/U_{red}))$ with $U_{red} = 5.0$.

From figure 3 we observe that the critical Reynolds numbers for the single harmonic pulsatile waveforms at $Re \approx 389$ when $U_{ref} = 2.5$ ($\alpha = 15.6$), $Re \approx 415$ when $U_{red} = 5.0$ ($\alpha = 11.4$) and $Re \approx 500$ when $U_{red} = 10.2$. For the two harmonic waveform we observe a critical Reynolds number of $Re \approx 437$ when $U_{red} = 5.0$ ($\alpha = 11.7$).

Discussion and Conclusions

From the results we have observed that the linearised instability of the flow in a 75% axisymmetric stenosis occurs at a Reynolds number of $Re = 722$ when the flow is steady and between $389 \leq Re \leq 500$ for the pulsatile waveforms considered. The unstable mode was completely real indicating a stationary instability at $\beta = 1$. The steady flow critical Reynolds number is relatively high for normal physiological conditions in the systemic or coronary arteries. However in an axisymmetric stenosis the sectional Reynolds number increases as the inverse of the local diameter. We might therefore expect that higher degrees of stenosis (i.e greater reduction of diameter) would lead to a reduction of the critical Reynolds number.

The introduction of unsteadiness into the base flow has led to a reduction in the critical Reynolds number as compared to the steady base flow case. For the single harmonic waveforms considered we have a peak to mean ratio of Q_{p2m} of 1.75. Although this implies that the peak Reynolds number of the flow is similar in magnitude to that of the instability of the steady flow case, we do not believe that the mechanisms are similar. This is partly supported by the differences in the base flow characteristics. For the steady flow we observe a single, large recirculation ring behind the stenosis. In contrast, for the pulsatile flow we observe a series of ring vortices which are generated just after the stenosis and then advected downstream whilst reducing in magnitude as they interact with the pipe wall. The unsteady instability is also associated with a period doubling phenomenon which is not possible in the steady flow case. The introduction of the two harmonic waveform allowed the peak to mean ratio to be increased to $Q_{p2m} = 2.25$ and represents a more realistic physiological waveform. However despite the increase in peak Reynolds number for this case we observe an increase, rather than the expected reduction, in the critical Reynolds number for onset of instability as compared to the single harmonic waveform at $U_{red} = 5.0$.

In addition to the linearised stability analysis we have perform direct numerical simulations at mildly unstable Reynolds numbers for both the steady and unsteady stenotic flows. These simulations have supported the linearised analysis and also demonstrated that the flow becomes transitional in a very localised manner at approximately $15D$ downstream of the stenosis.

Future work. Using BiGlobal analysis we are able to cover a wide range of parameters to understand the mechanisms behind the transition to three-dimensional weakly turbulent flow due to stenotic obstructions. This type of transition is significant since it generates unsteady temporal and spatial wall shear stress gradients that are implicated in the onset of atherosclerosis. The flow features observed may further help explain the occurrence of multiple stenosis. Currently we are investigating the effect of multiple harmonics in order to analyse more physiologically realistic waveforms. A final extension to this work is to introduce geometry or inflow asymmetry into the base flow to understand the important effect of these modifications on the stability of the flow.

Acknowledgements

The first author would like to acknowledge the partial support from a Global Research Award from the Royal Academy of Engineering. We would also like to acknowledge computing facilities from the Australian Partnership for Advanced Computing (APAC) national facilities.

*****

References

[1] S.A. Berger and L.-D. Jou. Flow in stenotic vessels. *Ann. Rev. Fluid Mech.*, 32:347–384, 2000.

[2] R. Pitt, S.J. Sherwin, and V. Theofilis. Biglobal stability analysis of stenotic flow. In *Proceeding of Turbulence and Shear Flow Phenomena*, pages 787–791, Sendai, Tokoyo, 2003.

[3] H.M. Blackburn and J.M. Lopez. Symmetry breaking of the flow in a cylinder driven by a rotating endwall. *Phys. Fluids*, 12(11):2698–2701, 2000.

[4] D.Barkley and R.D. Henderson. Floquet stability analysis of the periodic wake of a circular cylinder. *J. Fluid. Mech.*, 8:1683, 1996.

[5] L.S. Tuckerman and D. Barkley. *Bifurcation Analysis for Time-Steppers*, pages 543–566. Numerical Methods for Bifurcation Problems and Large-Scale Dynamical Systems (eds. E. Doedel and L.S. Tuckerman. Springer, New York, 2000.

[6] G.E. Karniadakis, M. Israeli, and S.A. Orszag. High-order splitting methods for incompressible Navier-Stokes equations. *J. Comp. Phys.*, 97:414, 1991.